



Geomorphological evidence for transient water flow on Vesta



Jennifer E.C. Scully^{a,*}, Christopher T. Russell^a, An Yin^a, Ralf Jaumann^b, Elizabeth Carey^c, Julie Castillo-Rogez^c, Harry Y. McSween^d, Carol A. Raymond^c, Vishnu Reddy^{e,f}, Lucille Le Corre^f

^a Department of Earth, Planetary, and Space Sciences, University of California, Los Angeles, 595 Charles Young Drive East, Box 951567, Los Angeles, CA 90095-1567, USA

^b Institute of Planetary Research, German Aerospace Center (DLR), Rutherfordstraße 2, 12489 Berlin, Germany

^c Jet Propulsion Laboratory, California Institute of Technology, 4800 Oak Grove Drive, Pasadena, CA 91109, USA

^d Department of Earth and Planetary Sciences, 1412 Circle Drive, University of Tennessee, Knoxville, TN 37996-1410, USA

^e Max Planck Institute for Solar System Research, Justus-von-Liebig-Weg 3, 37077 Göttingen, Germany

^f Planetary Science Institute, 225 South Lake Avenue, Tucson, AZ 85719, USA

ARTICLE INFO

Article history:

Received 10 June 2014

Received in revised form 14 November 2014

Accepted 2 December 2014

Available online 19 December 2014

Editor: C. Sotin

Keywords:

Vesta
geomorphology
gullies
lobate deposits
transient water flow
volatiles

ABSTRACT

Vesta, the second most massive asteroid, has long been perceived as anhydrous. Recent studies suggesting the presence of hydrated minerals and past subsurface water have challenged this long-standing perception. Yet, direct geologic indications of water activity on Vesta's surface were unexpected. Herein we show evidence that transient water flowed on the surface, in a debris-flow-like process, and left distinctive geomorphologic features. Based on detailed analysis of highest-resolution (~20 m/pixel) images obtained by the Dawn spacecraft, we identify a class of locally occurring, interconnected and curvilinear gully networks on the walls of young (< hundreds of Ma) impact craters, ending in lobate deposits near the crater floors. As curvilinear systems only occur within impact craters, we propose that they formed by a particulate-dominated flow of transient water that was released from buried ice-bearing deposits by impact-induced heating and melting. This interpretation is in accordance with the occurrence of pitted terrain on lobate deposits and crater floors. Pitted terrain is proposed to result from the degassing of volatiles. The proposed buried ice-bearing deposits are likely localized in extent and may be currently extant in Vesta's subsurface. Together with the discovery of water evaporation on Ceres and water activity on several small asteroids, our results support the new paradigm that water is widespread in the asteroid belt.

© 2014 Elsevier B.V. All rights reserved.

1. Introduction

1.1. Vesta and the Dawn mission

Vesta, with a mean radius of 262.7 ± 0.1 km, is the second most massive asteroid and is located in the asteroid belt at ~2.15–2.57 AU (e.g. Russell et al., 2012). Data from the Dawn mission confirmed the basaltic HED (howardite–eucrite–diogenite) meteorites originate from Vesta (Russell et al., 2012; De Sanctis et al., 2012; Prettyman et al., 2012; Reddy et al., 2012b). Vesta is

called a protoplanet because it differentiated ~4.56 bya to form a core, mantle and crust, but did not become a terrestrial planet (e.g. Russell et al., 2012; McSween et al., 2011). Vesta's differentiation and size make it a unique world, with characteristics residing between those of larger, differentiated rocky bodies and smaller, non-differentiated asteroids. Impacts on Vesta have lower velocities than on the terrestrial planets, since Vesta has a lower surface gravity (0.25 m/s^2 versus 9.81 m/s^2 for Earth and 3.71 m/s^2 for Mars). As a result, substantially less silicate impact melt is produced by impacts on Vesta than by similarly-sized impacts on the terrestrial planets; this is confirmed by mapping and modeling calculations (Williams et al., 2014a).

Vesta has been called "... the smallest of the terrestrial planets" (Keil, 2002), which is consistent with the Dawn mission's discovery that Vesta is a heterogeneous and complex mini-world, home to many planetary-type processes (e.g. Russell et al., 2014). Planetary-type graben are formed by impact-induced stresses

* Corresponding author. Tel.: +1 310 794 5385.

E-mail addresses: jscully@ucla.edu (J.E.C. Scully), ctrussel@igpp.ucla.edu (C.T. Russell), yin@ess.ucla.edu (A. Yin), ralf.jaumann@dlr.de (R. Jaumann), Elizabeth.M.Carey@jpl.nasa.gov (E. Carey), julie.c.castillo@jpl.nasa.gov (J. Castillo-Rogez), mcsween@utk.edu (H.Y. McSween), carol.a.raymond@jpl.nasa.gov (C.A. Raymond), reddy@psi.edu (V. Reddy), lecorre@psi.edu (L. Le Corre).

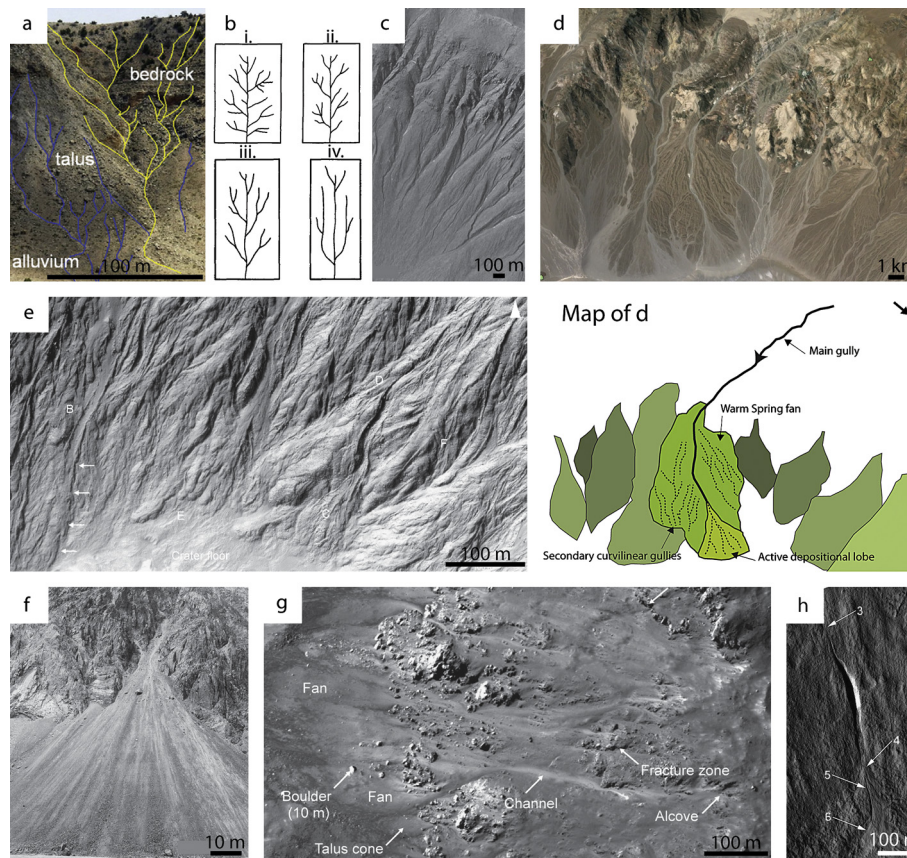


Fig. 1. Gullies and lobate deposits on Earth, Mars and the Moon. (a) Networks of gullies formed by flow of water in Meteor Crater (from Kumar et al., 2010). Yellow-colored gullies incise into bedrock and blue-colored gullies incise into talus and alluvium. The gullies have sub-dendritic to sub-parallel drainage patterns (see b). (b) Drainage patterns: (i) dendritic; (ii) sub-dendritic; (iii) sub-parallel; (iv) parallel. Flow of water on shallower slopes (less than a few degrees) forms dendritic patterns and flow of water on steeper slopes (greater than a few degrees) forms sub-dendritic to sub-parallel patterns (from Phillips and Schumm, 1987). (c) The first gullies observed on Mars have an alcove source region, incised curvilinear and interconnected channels and depositional aprons; they were first interpreted to form from water flow sourced in the subsurface (from Malin and Edgett, 2000). Additional alternative formation mechanisms have since been proposed (see Section 1.2). (d) Unmapped and mapped versions of alluvial fans in Death Valley, California (based on Blair, 1999; image credit: Google Earth). The Warm Spring fan is a lobate-shaped deposit sourced by an incising main curvilinear gully (solid black line); the deposit contains incised secondary gullies (dashed black lines) and individual lobes, for example the active depositional lobe. The multiple cross-cutting and coalescing alluvial fans (shades of green) form a bajada deposit. (e) Deposits with overlapping lobes and incised gullies within Istok crater on Mars, interpreted as debris flow deposits (from Johnsson et al., 2014). (f) Terrestrial talus cone with no individual lobes or incised gullies, interpreted to form by dry granular flow (from Johnsson et al., 2014). (g) Lunar gullies are linear, parallel, non-intersecting channels that only sometimes incise the bedrock and end in talus deposits that do not have individual lobes or incised gullies. They are interpreted to form by dry granular flow (from Kumar et al., 2013). (h) Surficial gully on Mars. Martian surficial gullies do not originate in alcoves, are more shallowly incised into the crater walls than the gullies in (a), (c) and (d) and end in depositional fans (from Schon and Head, 2011, 2012). (For interpretation of the references to color in this figure legend, the reader is referred to the web version of this article.)

(Buczkowski et al., 2012; Jaumann et al., 2012; Scully et al., 2014) and the surface exhibits compositional diversity, with exogenous, carbonaceous chondrite deposits (Reddy et al., 2012a; McCord et al., 2012), olivine (Ammannito et al., 2013), and hydrated minerals (De Sanctis et al., 2012; Prettyman et al., 2012). Furthermore, there is evidence of intrusive mantle-derived magmatic activity (Buczkowski et al., 2014; De Sanctis et al., 2014; Raymond et al., 2013). Additionally, similar to the Earth, Mars and the Moon, systems of gullies form on the surface of Vesta.

In this paper, Section 1.2 overviews analogous features; Section 2 outlines our methods; Section 3 details our observations of gully systems; Section 4 considers possible formation mechanisms of gully systems; Section 5 tests our hypothesis through quantitative modeling and experiments; and Section 6 discusses implications and conclusions.

1.2. Gullies and lobate deposits in the solar system

In order to understand gullies on Vesta, we first consider their formation on other bodies. On Earth, gullies are defined as ephemeral channels that carry water for short periods of time. For example, sub-dendritic to sub-parallel drainage patterns of curvi-

linear gullies form by flow of water on the steep crater-wall slopes of Meteor Crater, Arizona (e.g. Kumar et al., 2010) (Fig. 1a). The gullies in Meteor Crater illustrate the tendency of channels formed by flow of water on steeper slopes ($>2\text{--}3\%$) to become more parallel and less dendritic in pattern (Phillips and Schumm, 1987) (Fig. 1b).

Many of the gullies observed on Mars are also located within impact craters (e.g. Carr, 2012). The first gullies observed on Mars consist of an alcove source region, curvilinear and interconnected channels, and depositional aprons (Malin and Edgett, 2000) (Fig. 1c). These original gullies were interpreted to result from water flow sourced in the subsurface (Malin and Edgett, 2000). However, many gully morphologies have since been identified, and alternate formation mechanisms proposed, including: water from melting of subsurface water–ice (e.g. Schon and Head, 2012, 2011; Mellon and Phillips, 2001), water from melting of frost and snow (e.g. Reiss et al., 2010; Hauber et al., 2011), flow of brines (e.g. Knauth and Burt, 2002), flow of liquid CO_2 (e.g. Musselwhite et al., 2001), CO_2 frost (e.g. Diniega et al., 2010; Dundas et al., 2012), CO_2 vapor-supported flows (e.g. Stewart and Nimmo, 2002), frosted granular flow (e.g. Hugenholz, 2008) and

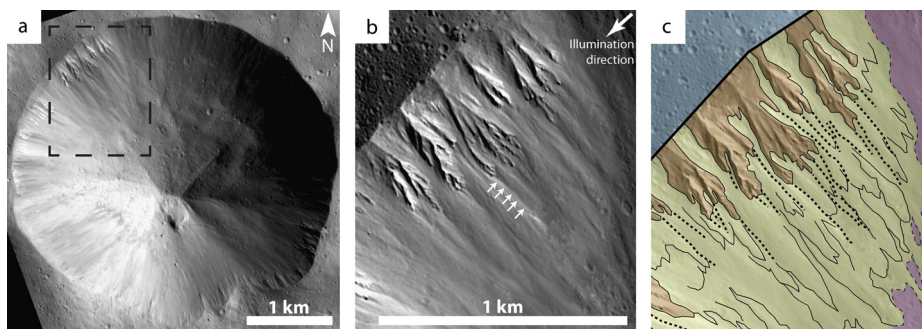


Fig. 2. Example of a linear system. (a) Fonteia crater, in which the example linear system occurs. The dashed box shows the location of (b). (b)–(c) Unmapped (b) and mapped (c) versions of a linear system in the northwestern crater wall of Fonteia. The direction of illumination is from the northeast, thus the linear gullies have shadows on their northeastern sides and are illuminated on their southwestern sides. The linear gullies (black dashed lines) are straight, non-intersecting, parallel to one another, and originate from alcoves directly below spurs on the crater rims (orange unit). White arrows delineate the path of a particular linear gully in (b). Linear gullies are topographic depressions formed by the intersection of talus deposits (yellow unit; individual deposits outlined by black solid lines) that do not contain incised gullies or individual lobes. (For interpretation of the references to color in this figure legend, the reader is referred to the web version of this article.)

dry flow of eolian material (e.g. Treiman, 2003) or of CO₂ blocks (e.g. Diniega et al., 2013).

Many gullies on Earth and Mars end in lobate-shaped deposits. For example, terrestrial gullies, in Death Valley, California, are the sources of lobate-shaped alluvial fan deposits (Blair, 1999). These can be formed by flows with $\geq 30\%$ water content or by debris flows with $\leq 30\%$ water content. The main gully in Fig. 1d ends in a lobate-shaped alluvial fan deposit, called the Warm Spring fan. This fan is formed by debris flow processes because of the nature of the particles in the source region; they are unsorted with a variety of sizes and a high concentration of fine grains. These conditions allow for water to become easily trapped in pore spaces and for pore pressures to increase, mobilizing the particles into a debris flow (Blair, 1999). The main gully is curvilinear, is incised into the bedrock and also incises the fan surface. This main gully feeds into the most recently active part of the fan, called the active depositional lobe, which is an individual lobe visible at the toe of the alluvial fan. Many secondary curvilinear gullies, some of which interconnect with each other, also incise the fan surface. A number of other gullies also terminate in lobate-shaped alluvial fans, which cross-cut and coalesce with one another to form a bajada deposit (Fig. 1d).

Johnsson et al. (2014) use the characteristic morphology of terrestrial gullies and lobate deposits formed by debris flow processes to argue that gullies and lobate deposits within Istok crater on Mars are formed by debris flows. Similar to the Death Valley example, gullies incise the martian lobate deposits and individual lobes are visible within the lobate deposits (Fig. 1e). Johnsson et al. (2014) further argue that the debris flow deposits are different from deposits formed by dry granular flow, called talus cones. Talus cones do not have incised gullies and do not display individual lobes (Fig. 1f).

Dry granular flow is proposed as the formation mechanism for gullies and talus deposits on the Moon (e.g. Kumar et al., 2013). These gullies only sometimes incise the bedrock (Kumar et al., 2013), are more linear than terrestrial and martian gullies, are parallel to one another and rarely intersect (Fig. 1g). They also end in talus cones/fan deposits that do not contain incised gullies or individual lobes. In order to characterize the formation mechanism of the vestan gullies and lobate deposits, we undertook detailed mapping to distinguish the presence or absence of the above features, which are indicative of water-based flow or dry granular flow.

2. Methods: mapping

Our work is mainly based on analysis of clear filter images taken by the Dawn Framing Camera (FC, Sierks et al., 2011) during the Low Altitude Mapping Orbit (LAMO), because of their high

spatial resolution of ~ 20 m/pixel. Yet, these highest spatial resolution Dawn images are ~ 1 – 2 orders of magnitude lower resolution than the martian, terrestrial and lunar images in Fig. 1. Thus, gullies and lobate deposits on Vesta are not as finely resolved as the features in Fig. 1.

We obtain compositional data from hyperspectral images from 0.25–5.1 μm , recorded by the Visible and Infrared Spectrometer (VIR) (De Sanctis et al., 2011). Moreover, further compositional information is provided by Clementine-type ratio images of the FC's color filters (Reddy et al., 2012b). Additionally, shape models derived from the FC data by stereophotogrammetry (~ 100 m/pixel resolution, Preusker et al., 2012) and by stereophotoclinometry (~ 50 m/pixel resolution, Gaskell, 2012) are used.

Examination and mapping of gully systems and lobate deposits is carried out with the use of ESRI ArcMap 10.0 software, which facilitates georeferenced mapping. Moreover, the USGS ISIS (Integrated Software for Imagers and Spectrometers) and JMARS (for Vesta), developed by ASU's Mars Space Flight Facility, are used to obtain topographic profiles from the shape models. However, many of the features under investigation are not clearly visible in the topographic profiles due to their low relief; i.e. their relief is < 50 m/pixel. Thus, we commonly identified a feature as being incised or protruding due to comparison of shadow locations with shadow locations in nearby features; for example, we compared the locations of shadows within nearby impact craters, which are clearly concave features, with the locations of shadows within possible gullies.

3. Observations

3.1. Overview

Systematic analysis of Dawn FC images identified 170 sites that could potentially contain gullies. Since gullies are most likely to be identifiable on young, sloping regions that have not been obscured by large accumulations of mass-wasted material, the 170 sites consist of impact craters and steep slopes with a fresh appearance. Of these 170 potential sites, 59 display gullies. We group gullies into two classes: linear systems at 51 sites (Fig. 2) and curvilinear systems at 8 sites (Figs. 3–5). Curvilinear systems are further subdivided into complete curvilinear systems (3 sites) (Figs. 3 and 4) and incomplete curvilinear systems (5 sites) (Fig. 5).

3.2. Linear systems

3.2.1. Morphology of linear systems

Linear systems contain straight, non-intersecting gullies that are parallel to one another (Fig. 2). They occur on crater walls, or on

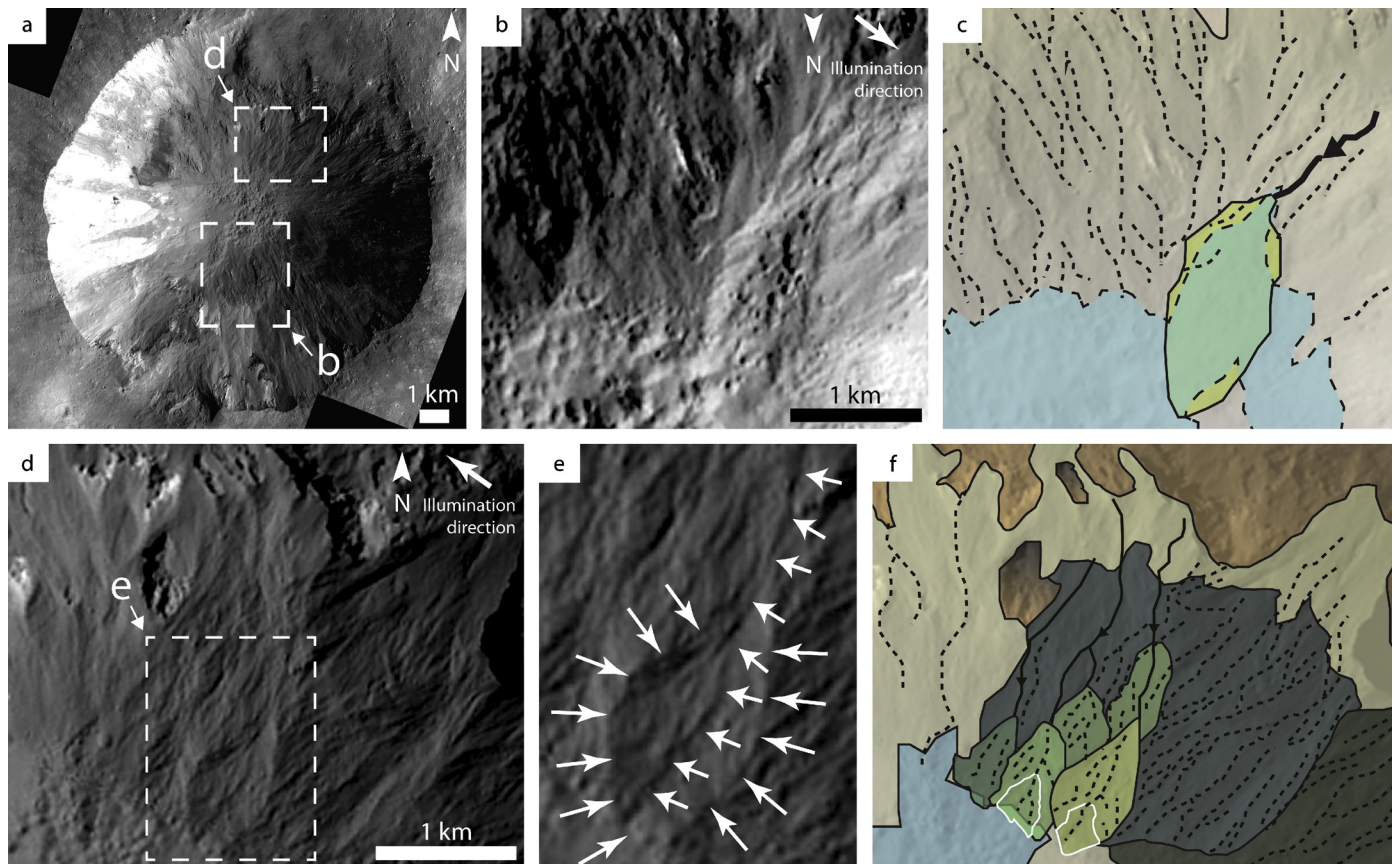


Fig. 3. Example of a complete curvilinear system. (a) Cornelia crater, in which the example complete curvilinear system occurs. The dashed white boxes show the locations of (b) and (d). (b)–(f) Unmapped (b), (d) and mapped (c), (f) versions of areas of complete curvilinear systems in Cornelia crater. The direction of illumination is from the southeast, thus the curvilinear gullies have shadows on their southeastern sides and are illuminated on their northwestern sides; the lobate deposits have shadows on their northwestern sides and are illuminated on their southeastern sides. Note that (a), (d), (e), and (f) are oriented with north to the top but that (b)–(c) are oriented with south to the top. Curvilinear gullies (black dashed lines) are non-linear, interconnected and form the sub-dendritic and sub-parallel patterns of Phillips and Schumm (1987). In (e), short white arrows delineate the path of a particular curvilinear gully, and long white arrows outline a lobate deposit. Curvilinear gullies originate in and shallowly incise the upper and middle sections of the crater walls (yellow unit) and some curvilinear gullies (black solid line with arrow showing inferred direction of flow) end in lobate deposits (green units) at the bottom of the crater walls. Lobate deposits are shallowly incised by curvilinear gullies and contain possible individual lobes (white outline in (f)). Lobate deposits partially overlie and coalesce with one another, reminiscent of terrestrial bajada deposits. Pitted terrain (blue unit) is found on the floor of Cornelia and also on some lobate deposits. (For interpretation of the references to color in this figure legend, the reader is referred to the web version of this article.)

slopes outside of craters, and originate from alcoves directly below spurs on the crater rims. Spurs are blocky accumulations of material that protrude from the slope surfaces. Individual linear gullies mark boundaries between deposits of talus, which likely result from mass wasting of material in the downslope direction. Thus, the topographic depressions expressed as linear gullies do not result from incisional erosive processes, but from the intersection of depositional talus deposits. The talus deposits appear to be homogenous and do not contain incised gullies or individual lobes.

3.2.2. Analogs to linear systems

The vestan linear gullies have certain features that are analogous to those of the lunar gullies (Fig. 1g) (see Section 1.2): both are linear, parallel to one another and rarely interconnect. Also, talus deposits, adjacent to the vestan linear gullies and at the end of lunar gullies, are similar to terrestrial talus cones (Fig. 1f) because they lack incised gullies or individual lobes.

3.3. Curvilinear systems

Since complete curvilinear systems are the ideal examples of curvilinear systems, we discuss their morphology first (Section 3.3.1), followed by the incomplete curvilinear systems (Section 3.3.3).

3.3.1. Morphology of complete curvilinear systems

Complete curvilinear systems consist of interconnected, non-linear gullies that are particularly well-developed in Cornelia crater (Fig. 3) and in Marcia crater (Fig. 4). Their map-view patterns resemble sub-dendritic and sub-parallel drainage networks (Fig. 1b), consistent with their formation on steeply sloping crater walls (Phillips and Schumm, 1987). Curvilinear gullies do not originate in alcoves but in the upper-middle sections of crater walls, and terminate in lobate-shaped deposits near the base of the walls (Figs. 3 and 4). Each lobate deposit is sourced by a main curvilinear gully, which shallowly incises into the crater wall and the lobate deposits. Other partially interconnecting curvilinear gullies also shallowly incise the lobate deposits. Individual lobes may be identified within the lobate deposits and cross-cutting and coalescing of the lobate deposits is reminiscent of bajada deposits on Earth (Fig. 1d).

3.3.2. Age-dependence of preservation

We interpret the state of preservation of curvilinear systems to be age-dependent, illustrated by the curvilinear systems observed in the neighboring Marcia and Calpurnia craters. Morphological analyses have identified Marcia as being younger than Calpurnia and crater size-frequency ages suggest that Marcia is approximately one-quarter the age of Calpurnia (Hiesinger et al., 2014; Williams et al., 2014b). Younger Marcia hosts well-preserved sys-

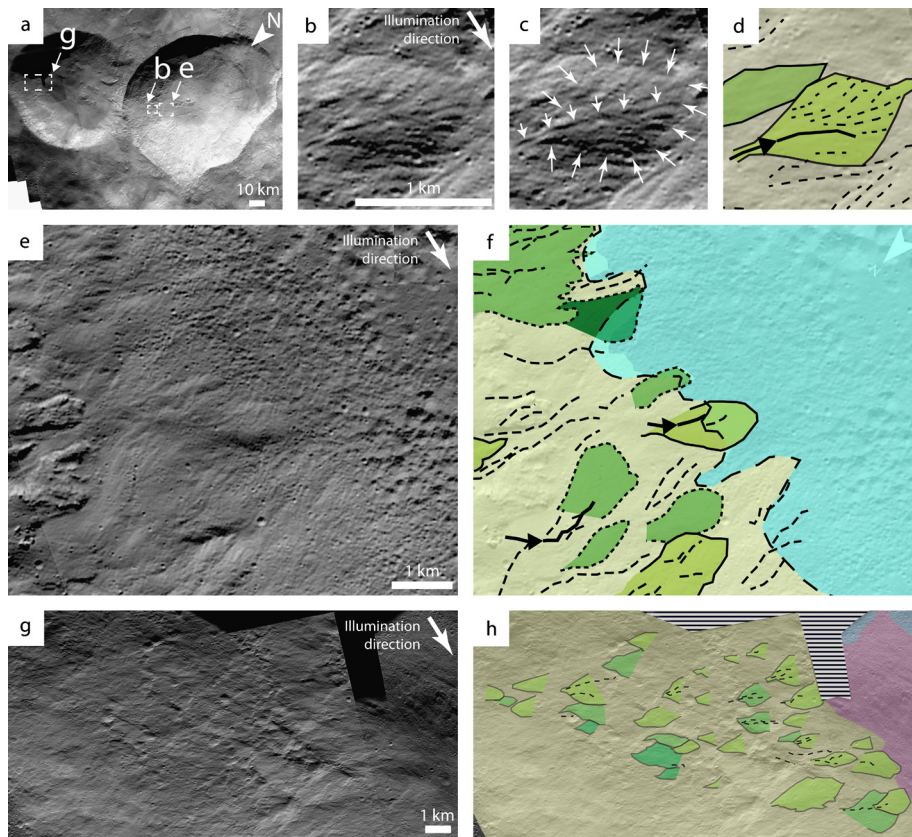


Fig. 4. Examples of well-preserved and less well-preserved complete curvilinear systems. (a) Calpurnia (left) and Marcia (right) craters, in which the example complete curvilinear systems occur. Marcia must be the older crater because its rim cross-cuts the expected path of the rim of Calpurnia. The dashed white boxes show the locations of (b), (e) and (g). In all images the direction of illumination is from the east, thus the curvilinear gullies have shadows on their eastern sides and are illuminated on their western sides; the lobate deposits have shadows on their western sides and are illuminated on their eastern sides. (b)–(d) Unmapped (b) and mapped (d) versions of a well-developed lobate deposit (pale green) in Marcia crater. In (c), short white arrows delineate the path of the main curvilinear gully, and long white arrows outline the lobate deposit. The lobate deposit is sourced by a main, shallowly incised, curvilinear gully (black solid line with arrow showing inferred direction of flow) and contains secondary, shallowly incised curvilinear gullies (dashed black lines). (e)–(f) Unmapped (e) and mapped (f) versions of well-developed curvilinear gullies (black lines) and lobate deposits (shades of green) in Marcia crater. The lobate deposits partially overlie and coalesce with one another and pitted terrain (blue) is visible on the crater floor and on top of some of the lobate deposits. (g)–(h) Unmapped (g) and mapped (h) part of the Calpurnia crater wall, which contains less well-developed complete curvilinear systems. There are a few, short curvilinear gullies (black dashed lines) and the lobate deposits (shades of green) are only partially complete and are more isolated from one another than in Cornelia (see Fig. 3) and Marcia craters. (For interpretation of the references to color in this figure legend, the reader is referred to the web version of this article.)

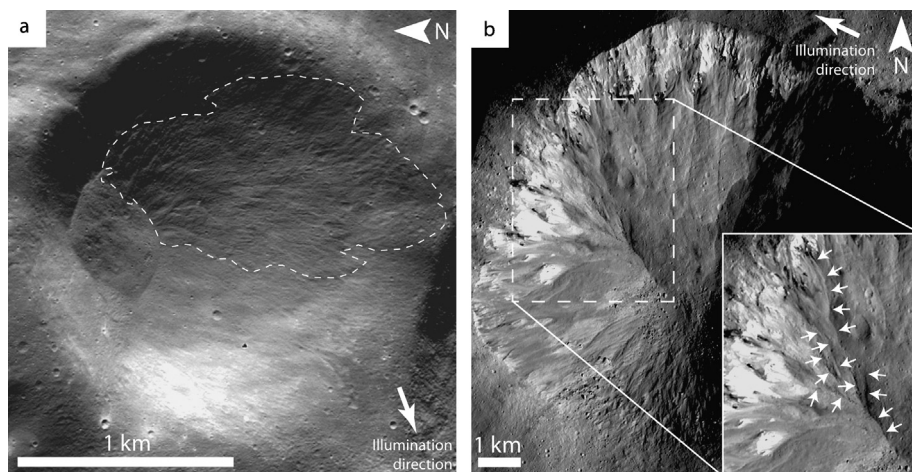


Fig. 5. Examples of incomplete curvilinear systems in Minucia (a) and Rubria (b) craters. (a) Superposed lobate deposits (outlined by the white dashed line) in Minucia crater lack interconnected gullies and appear to be lozenge or half-lozenge shaped; the superposition has obscured the true shape of each individual deposit. Similar deposits are observed in the walls of Caparronia and Teia craters and all three craters do not contain pitted terrain. (b) Curvilinear gullies lacking lobate deposit terminations in Rubria crater are outlined by the white box and are delineated by white arrows in the inset image. The interconnected gullies resemble gullies in complete curvilinear systems but form less developed networks because they do not end in lobate deposits. Incomplete curvilinear systems such as these also occur in Arruntia crater, and both craters lack pitted terrain.

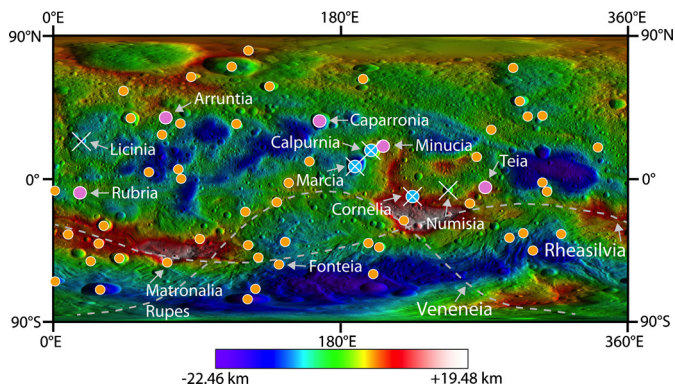


Fig. 6. Locations of linear and curvilinear systems. The background map is a shape model of Vesta relative to a reference ellipsoid of 285 km × 285 km × 229 km (Gaskell, 2012). Blue dots show craters containing complete curvilinear systems, pink dots show craters containing incomplete curvilinear systems and orange dots show craters and slopes with linear systems. White crosses (×) show craters containing pitted terrain. Craters containing curvilinear systems are clustered into two groups: in equatorial to mid-northerly latitudes from ~15–75°E and from ~170–270°E. In contrast, the linear systems are more evenly distributed across the vestan surface. Dashed grey lines show the outlines of the Rheasilvia and Veneneia impact craters. Curvilinear systems are not present in the Rheasilvia and Veneneia impact craters. (For interpretation of the references to color in this figure legend, the reader is referred to the web version of this article.)

tems, with clearly identifiable curvilinear gullies and lobate deposits, whereas the older Calpurnia hosts less well-preserved systems, with fewer curvilinear gullies and many partially complete lobate deposits (Fig. 4). We propose that modification of the original morphology by later geologic processes, such as infilling of gullies by mass wasting, is more developed in the older Calpurnia crater, because these processes have had more time to occur in the older Calpurnia crater.

3.3.3. Morphology of incomplete curvilinear systems

We find that incomplete curvilinear systems have some, but not all, elements of complete curvilinear systems. They consist of superposed lobate deposits lacking interconnected gullies (Fig. 5a), or of curvilinear gullies lacking lobate deposits (Fig. 5b). The missing portions appear to result from incomplete preservation, burial by younger geological processes and/or less availability of source material than for complete curvilinear systems (possible source materials are discussed in Section 4).

3.3.4. Pitted terrain

Pitted terrain is observed in five craters on Vesta (Denevi et al., 2012) (Fig. 6) and is morphologically similar to martian pitted terrain (Mouginis-Mark and Garbeil, 2007). Pitted terrain on Mars is interpreted to form by degassing of volatiles induced by impact heating (Mouginis-Mark and Garbeil, 2007); due to the morphological similarity, vestan pitted terrain is also proposed to form in this way (Denevi et al., 2012). Degassing pipes in the Ries crater, Germany (Newsom et al., 1986), are suggested as a terrestrial analog to pitted terrain (e.g. Tornabene et al., 2012). The Ries degassing pipes are observed in suevite deposits (Newsom et al., 1986), which are interpreted as silicate impact melt-bearing breccias emplaced as ground-hugging impact melt flows (e.g. Osinski, 2004). The degassing pipes are cylindrical structures formed as impact-released gases (at >500 °C) escaped through the fluidized suevite (Newsom et al., 1986). Thus, the roughly spherical pits that form pitted terrains are thought to be observations of cross sections of the ends of degassing pipes as they intersect the crater floor (e.g. Tornabene et al., 2012).

Our work indicates that all three craters hosting complete curvilinear systems also contain pitted terrain on their floors and sometimes on top of the lobate deposits (Figs. 3 and 4 and 6).

In contrast, craters hosting linear systems lack pitted terrain on their floors (Figs. 2 and 6). However, two craters containing pitted terrain do not contain curvilinear systems and all craters containing incomplete curvilinear systems do not contain pitted terrain (Figs. 5 and 6). This may be explained by burial by younger talus deposits or by a mechanism discussed in Section 4.3.3.

3.3.5. Analogs to curvilinear systems

The curvilinear systems on Vesta share many indicative features with curvilinear gullies and lobate deposits on Earth and Mars, including: complex, interconnected, sub-dendritic to sub-parallel drainage patterns of gullies; lobate-shaped deposits sourced by a main gully that is incised into the deposit and the bedrock/crater wall; partially interconnecting gullies and individual lobes within lobate deposits; and multiple cross-cutting and coalescing lobate deposits (see Section 1.2). However, we do not observe curvilinear gullies on Vesta to originate from an alcove and they appear to be more shallowly incised than many martian gullies (Fig. 1c) and terrestrial gullies (Fig. 1a).

As such, the morphology of vestan curvilinear gullies is reminiscent of the morphology of a specific set of young martian gullies, called surficial gullies (Schon and Head, 2012, 2011) (Fig. 1h). Although they form curvilinear channels and end in depositional aprons, surficial gullies have morphologies that are different to the original martian gullies (see Section 1.2); like the vestan curvilinear gullies they are more shallowly incised and sometimes originate in the crater walls without alcoves (Schon and Head, 2012, 2011). Surficial gullies are located in and around Gasa crater and are proposed to form by impact-induced flow of meltwater sourced in ice-rich mantle deposits and in buried glacier deposits, melted by the Gasa-forming impact. Nearby morphologies, such as polygonal textures, indicate the presence of ground ice (Schon and Head, 2012, 2011). It is possible that the martian surficial gullies and vestan curvilinear gullies are less incised because the flows that form them lasted for shorter periods of time.

3.4. Quantifiable geometrical properties of curvilinear systems and linear systems

We separate curvilinear gullies from linear gullies not only by morphology, but also by use of quantifiable geometrical parameters. For example, the length to width ratio of curvilinear gullies (on average ~30) is higher than the length to width ratio of linear gullies (on average ~13) (Fig. 7a). Similarly, curvilinear gullies have higher junction angles (~33° vs. ~16°) (Fig. 7b) and higher numbers of junctions (Fig. 7b) than linear gullies.

3.5. Distribution of locations of curvilinear and linear systems

We only observe linear systems on slopes outside of impact craters (e.g., at Matronalia Rupes) (Fig. 6). Locations of linear systems are also more evenly spread across the surface than locations of curvilinear systems and pitted terrain, which cluster into two general locations: in equatorial to mid-northerly latitudes from ~15–75°E and from ~170–270°E. Furthermore, we observe only linear systems in the two large impact craters in the southern hemisphere, Rheasilvia and Veneneia.

We also find that, within a given crater, the gullies are entirely linear systems or of a combination of both linear and curvilinear systems. Thus, craters defined to contain curvilinear systems (blue and pink dots in Fig. 6) also contain linear systems. As such, we never observe curvilinear systems in all segments of a crater, suggesting the factors responsible for forming curvilinear systems were localized within individual craters. Finally, we note that craters hosting gully systems and pitted terrain are young (< hundreds of Ma), as indicated by sharp rims, well-defined

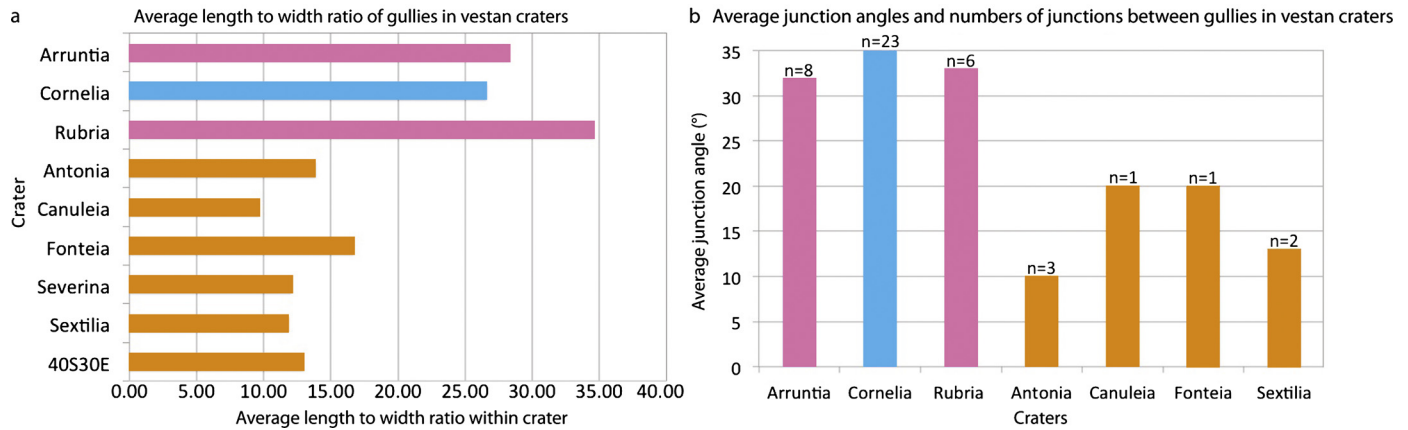


Fig. 7. Blue bars are complete curvilinear systems, pink bars are incomplete curvilinear systems and orange bars are linear systems. (a) Plot showing the average length to width ratios (x -axis) of gullies within a selection of vestan craters (y -axis). The average length to width ratio of curvilinear gullies, ~ 30 , is higher than the average length to width ratio of linear gullies, ~ 13 . (b) Plot showing the average junction angles (y -axis) and the number of junctions ($n = \#$, on top of bars) of gullies within a selection of vestan craters (x -axis). Gullies in linear systems intersect significantly less than gullies in curvilinear systems. When linear gullies do intersect the junction angles are lower (on average $\sim 16^\circ$) than those between gullies in curvilinear systems (on average $\sim 33^\circ$). (For interpretation of the references to color in this figure legend, the reader is referred to the web version of this article.)

crater-wall morphologies and crater size-frequency ages (Hiesinger et al., 2014; Williams et al., 2014b).

4. Interpretations: formation mechanisms

In this section we discuss possible formation mechanisms of the curvilinear and linear gullies, which we find to have contrasting morphologies through morphologic analysis and measurement of geometrical properties (see Section 3).

4.1. Silicate impact melt

We consider silicate impact melt to be the least likely agent for creating either gully type, firstly because of the low production of silicate impact melt on Vesta (see Section 1.1) and also because their shapes and patterns are inconsistent with gullies formed by silicate impact melt; for example, gullies formed by silicate impact melt on Earth's Moon have rounded levees, hummocky surfaces, globular lobes and spiral-flow patterns (e.g. Bray et al., 2010). Moreover, 'orange' areas in Clementine-type ratio images have been identified as silicate impact melts (Le Corre et al., 2013), and neither gully type occurs in these areas.

Furthermore, the surface temperatures (Appendix of Tosi et al., 2014), for example in the regions of Cornelia and Marcia craters containing curvilinear systems, are inconsistent with silicate impact melt. This is revealed by the difference in temperature between the pitted terrain in the crater floors (cooler at ~ 230 K) and the regions of curvilinear systems in the crater walls (hotter at ~ 240 – 260 K), when observed under the same conditions. The temperature difference implies that pitted terrain has a larger component of compacted silicate impact melt than the wall material, which is composed of less compacted regolith. The interpretation that pitted terrain is relatively rich in silicate impact melt is consistent with the occurrence of the terrestrial analog for pitted terrain, degassing pipes, in silicate impact melt-bearing breccias (see Section 3.3.4 and Tornabene et al., 2012; Osinski, 2004; Newsom et al., 1986).

4.2. Dry flow

Since the vestan linear gullies are straight, non-intersecting topographic depressions resulting from the intersection of homogeneous talus deposits, it is likely that they form by downslope dry mass wasting of material. This interpretation is supported by the

fact that certain features of vestan linear gullies are analogous to lunar gullies, which are also interpreted to form by dry granular flow (e.g. Kumar et al., 2013) (see Sections 1.2 and 3.2.2).

Although linear gully formation is consistent with dry granular flow, it is difficult to apply this same mechanism for curvilinear gully formation. This is because if both formed by dry granular flow, some factor is necessary to form their different morphologies, and we have identified no such factor. For example, morphology of drainage networks becomes more dendritic with decreasing surface slope (Phillips and Schumm, 1987), which could explain the more interconnected, sub-dendritic and sub-parallel networks of curvilinear gullies. However, both gully types occur on slopes between $\sim 15^\circ$ and $\sim 45^\circ$ (Fig. 8).

It is also possible that the difference in gully-network geometry is controlled by different composition of dry granular material. Yet, visual inspection reveals no association between the gully type and proportion of dark, bright, or gray material in a crater. Dark, bright and gray materials are the three main types of material on Vesta's surface (see Reddy et al., 2012b for details). Alternatively, curvilinear gullies could form by flow of material that is more finer grained in comparison to the material that formed linear gullies; comparatively finer grained dry material could flow like a liquid on bodies with gravity lower than Earth (Shinbrot et al., 2004). However, thermal inertia data (Capria et al., 2014) imply that material at curvilinear gully sites has comparatively coarser grain sizes than material at linear gully sites. Note that relative grain sizes, not specific grain size measurements, are derived by the work of Capria et al. (2014).

4.3. Transient water flow

Since we identified no factor that could explain dry flow forming both linear and curvilinear gullies, we investigate the possibility that the difference in gully morphology is due to variation in the composition and rheological properties of the flowing media. Specifically, we propose that linear gullies form by dry granular flow, whereas curvilinear gullies form by transient flow of liquid water in a debris-flow-like process.

4.3.1. Indications of hydrated minerals and subsurface water

This proposition is in accordance with meteorite and Dawn data indicating hydrated minerals and past subsurface water. For example, the VIR instrument detected a widespread, heterogeneous 2.8 μm OH absorption on Vesta's surface, attributed to hydrated

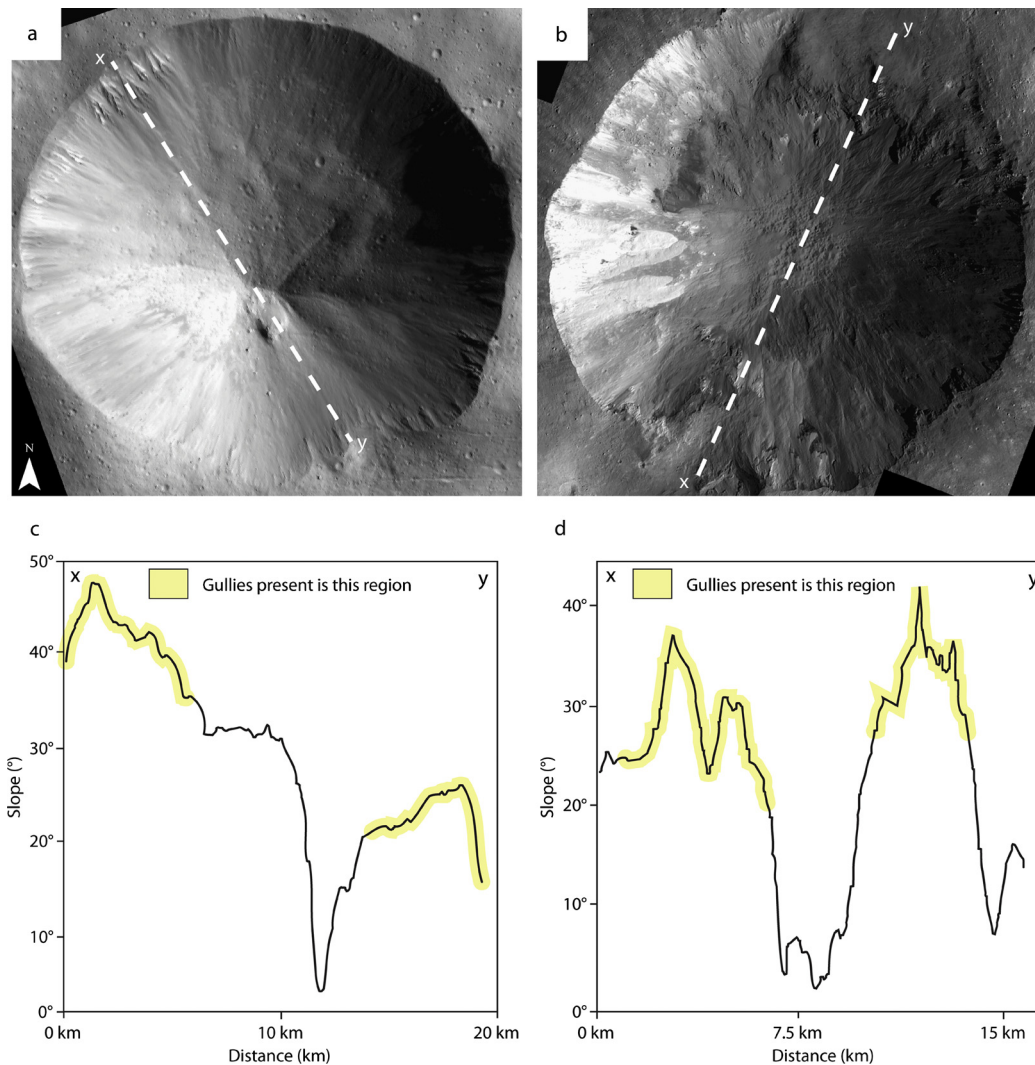


Fig. 8. Slope profiles of Fonteia (a), (c) and Cornelia (b), (d) craters. (a) Location of slope profile in Fonteia crater, which contains linear systems. (b) Location of slope profile in Cornelia crater, which contains curvilinear systems. (c) The regions of the walls in which the linear gullies occur (shaded yellow) have slopes ranging between $\sim 15^\circ$ and $\sim 45^\circ$. (d) The regions of the walls in which the curvilinear gullies occur (shaded yellow) also have slopes ranging between $\sim 15^\circ$ and $\sim 45^\circ$. (For interpretation of the references to color in this figure legend, the reader is referred to the web version of this article.)

minerals (De Sanctis et al., 2012). Similarly, Dawn's Gamma Ray and Neutron Detector (GRaND) finds that hydrogen, in excess of $400 \mu\text{g/g}$, corresponds to areas of carbonaceous chondrite and indicates the presence of mineralogically bound OH and/or H_2O (Prettyman et al., 2012). Additionally, mineralogically bound water is present in carbonaceous chondrite clasts in howardite meteorites from Vesta (Herrin et al., 2011) and Vesta's dark material is interpreted as deposits from carbonaceous chondrite impactors (McCord et al., 2012; Reddy et al., 2012a). Moreover, in a few eucrite meteorites from Vesta, quartz veins and other features are interpreted as deposits from aqueous solutions that percolated through the rocks (Warren et al., 2013; Barrat et al., 2011; Treiman et al., 2004). Some eucrites also contain apatites with high contents of mineralogically bound OH, indicating the localized presence of past interior water (Sarafian et al., 2013). On account of these data, we investigate flow of water as a formation mechanism of curvilinear systems instead of other fluids, such as carbon dioxide, which has been suggested as a possible formation mechanism for martian gullies (see Section 1.2).

4.3.2. Proposed source of transient water: dark material

Liquid water is unstable on Vesta's surface, due to the average temperature, $\sim 145 \text{ K}$ (Stubbs and Wang, 2012), and lack of an

atmosphere. Thus, transient water sources must be located elsewhere. We consider impact-induced devolatilization of carbonaceous chondrite as a potential liquid water source; impact-induced devolatilization has been proposed as a source of water vapor for the formation of pitted terrain (e.g. Denevi et al., 2014, 2012). We compared occurrences of dark material (mapped by Jaumann et al., 2014) within craters containing curvilinear systems to occurrences within craters containing linear systems. We found no systematic correlation between the number of occurrences of dark material and the type of gully system within a crater (Fig. 9). Furthermore, we also found no correlation between the source regions of curvilinear gullies and locations of dark material within Marcia and Cornelia craters. Therefore, our analysis, combined with a lack of evidence of the release of water in the liquid form by impact devolatilization, suggest that dark material is an unlikely source.

4.3.3. Proposed source of transient water: ice-bearing subsurface deposits

Alternatively, we propose discontinuously distributed ice-bearing deposits as the transient water source, because thermal models indicate water-ice could survive for billions of years if buried only a few meters deep (e.g. Stubbs and Wang, 2012). Craters containing incomplete curvilinear systems and no pit-

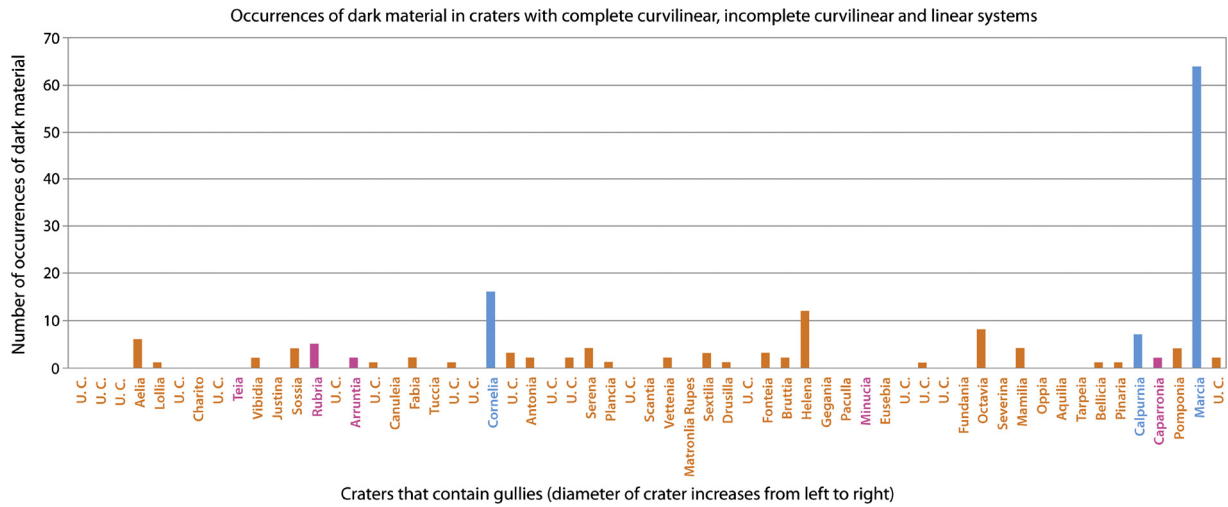


Fig. 9. Plot showing the number of occurrences of dark material within craters with complete curvilinear systems (blue columns), incomplete curvilinear systems (pink columns) and linear systems (orange columns). If dark material is the source of transient water that forms curvilinear systems, we would expect craters containing complete curvilinear systems to have the most dark material; craters containing linear systems to have the least dark material; and craters containing incomplete curvilinear systems to have an intermediate amount of dark material. This figure does not illustrate this relationship. For example, Calpurnia crater, which contains complete curvilinear systems, has less/equal amounts of dark material than some craters containing linear systems; and craters containing incomplete curvilinear systems frequently have less/equal amounts of dark material than many craters containing linear systems. Since there is no systematic correlation between the type of gully system within a crater and the number of occurrences of dark material within the crater, we regard carbonaceous chondrite dark material as an unlikely source of transient water. (For interpretation of the references to color in this figure legend, the reader is referred to the web version of this article.)

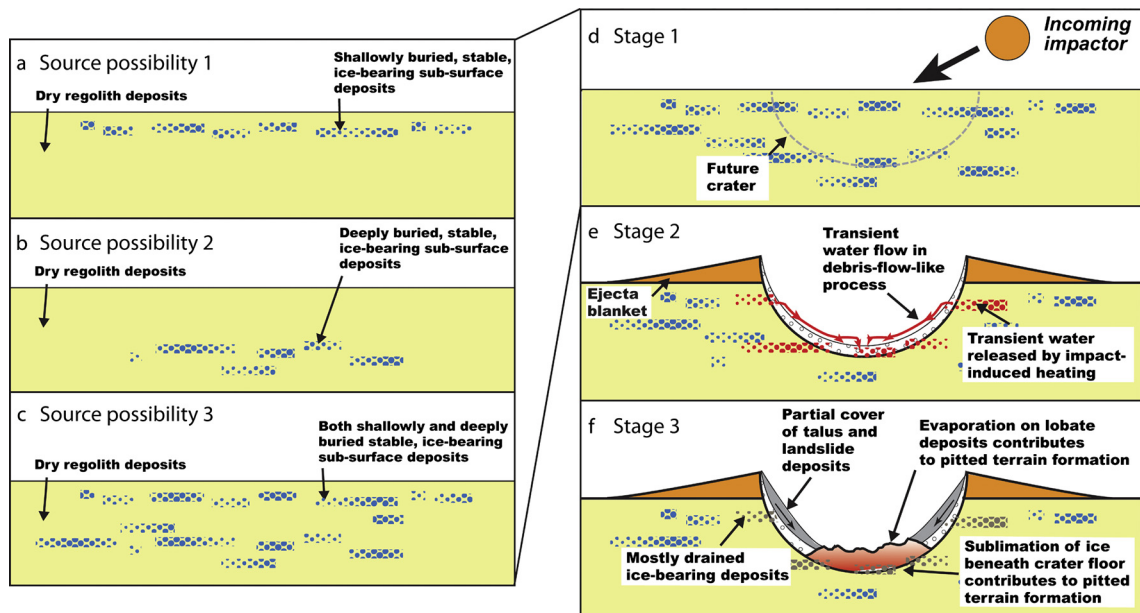


Fig. 10. Schematic diagram showing possible locations of ice sources (a)–(c) and the stages proposed to form the curvilinear systems (d)–(f). (a) Source possibility 1: ice-bearing subsurface deposits are only present at shallower levels. If impacted, incomplete curvilinear systems without pitted terrain will form in the walls of the crater. (b) Source possibility 2: ice-bearing subsurface deposits are only present at deeper levels. If impacted, pitted terrain without curvilinear systems will form in the crater floor. (c) Source possibility 3: ice-bearing subsurface deposits are present at both shallow and deep levels. If impacted, both curvilinear systems and pitted terrain will form in the crater, as detailed in (d)–(f). (d) Stage 1: an impactor provides the energy necessary to melt some of the shallow and deep ice-bearing subsurface deposits. (e) Stage 2: water is released onto the crater walls and flows transiently in a debris-flow-like process to the crater floor, forming the curvilinear gullies as it flows. (f) Stage 3: evaporation of water that remains after flow may contribute to the formation of the pitted terrain on lobate deposits. Sublimation of deep ice-bearing subsurface deposits may contribute to formation of pitted terrain on the crater floor.

ted terrain likely have a comparatively shallow ice-deposit source (Fig. 10a), since curvilinear systems originate in the upper-middle crater walls. Craters containing only pitted terrain likely have a deeper ice-deposit source (Fig. 10b), since pitted terrain occurs on the crater floors and lower walls. Craters containing both likely have both sources (Fig. 10c). Therefore, discontinuously distributed ice-bearing deposits explain the association between pitted terrain and complete curvilinear systems and disassociation between

pitted terrain and incomplete curvilinear systems, previously described in Section 3.3.4.

It is implausible that the crater-forming impactors of craters hosting curvilinear systems and pitted terrain were also the ice-bearing deposit sources, because it is improbable that ice-bearing impactors would all hit the two regions in which curvilinear systems and pitted terrain occur (Fig. 6). Consequently, we find that it is more probable that ice-bearing subsurface deposits were present in localized areas of these two regions before crater formation,

and are therefore older than the host craters, i.e. older than a few hundreds of Ma. This is consistent with the indication of >4.4 Ga subsurface water activity in Vesta from a eucrite meteorite (Treiman et al., 2004). We propose that speculative sources of the ice-bearing subsurface deposits are the retained fraction of > hundreds of Ma ice-rich impactors (Turrini and Svetsov, 2014) or, if partially preserved, an unmelted, primordial chondritic crust (Formisano et al., 2013; Fu and Elkins-Tanton, 2014).

4.3.4. Stages of proposed formation mechanism

4.3.4.1. Stage 1: Impact-induced melting of ice The lack of curvilinear systems within the Rheasilvia and Veneneia impact craters may result from total excavation and destruction of ice-bearing deposits during these large crater-forming events (Fig. 6). Rheasilvia and Veneneia are the largest impact craters on Vesta, with diameters of ~500 km and ~400 km respectively (Schenk et al., 2012). However, during impacts smaller than Rheasilvia and Veneneia, incomplete excavation to the ice-bearing deposit level may occur (Fig. 10d) and melt part of the ice-bearing deposits, releasing water for transient flow. We class smaller impacts as those that form craters </~70 km in diameter. This is the size of Marcia crater, which is the largest crater containing curvilinear systems. This mechanism is consistent with the lack of curvilinear systems outside of impact craters and consistent with energy calculations (see Section 5.1.1).

4.3.4.2. Stage 2: Transient flow of water in a debris-flow-like process The impact-released water would contain entrained particles from the regolith-rich crater wall and would begin to evaporate upon release. However, we hypothesize that not all of the water evaporated instantaneously and that water transiently flowed down the crater walls, in a debris-flow like process, to form curvilinear gully systems (Fig. 10e) (see Sections 5.1.2, 5.1.3 and 5.2 for further discussion). We propose that this transient flow was a debris-flow like process, containing ≤30% water, rather than a more water-rich flow (≥ 30%), because the regolith-rich wall of the newly formed crater would provide many of the conditions necessary to form a debris flow (see Section 1.2). For example, a wide variety of unsorted particle sizes with a high concentration of fine grains would be available for mobilization down the wall by the impact-released water.

4.3.4.3. Stage 3: Formation of pitted terrain Subsequently, evaporation of transient water remaining within lobate deposits may contribute to the formation of pitted terrain on lobate deposits (Fig. 10f). We further hypothesize that sublimation of deep-seated ice-bearing deposits contributed to creation of pitted terrain on crater floors (Fig. 10f) (see Sections 5.1.2, 5.1.3 and 5.2 for further discussion).

5. Quantitative modeling and experimental work

In order to test the plausibility of this hypothesis it is necessary to show that: (1) the volume of water required to form the curvilinear systems and pitted terrain could be released by impact-induced heating and (2) water could transiently survive on the surface for the time necessary to form the curvilinear systems. These two conditions are discussed in the following sections. Section 5.1 focuses on quantitative modeling and Section 5.2 focuses on experimental work. In Section 5.1 Cornelia crater is used as the basis for calculations, because due to its young age (Buczowski et al., 2014) Cornelia contains some of the best preserved examples of curvilinear systems.

5.1. Quantitative modeling

5.1.1. Energy

This calculation shows that the energy of the Cornelia-forming impactor is much greater than the energy needed to melt the requisite amount of ice to form the Cornelia curvilinear system. The approximate energy of the Cornelia-forming impactor is calculated from its approximated mass and velocity; the approximate mass is found by approximating the volume by use of the following equation, for sand or cohesive soil in the gravity regime (Holsapple and Housen, 2007):

$$R/a = 1.03(ga/U^2)^{-0.170}(\delta/\rho)^{0.332} \quad (1)$$

where R = final radius of Cornelia (7500 m); a = impactor radius; g = Vesta's gravitational acceleration (0.25 m/s^2); U = normal velocity component of impactor (4000 m/s; most probable velocity of impactors, O'Brien and Sykes, 2011); δ = density of impactor (3100 kg/m^3 , approximate average density of impactors, found from carbonaceous chondrite density, Britt and Consolmagno, 2004; and Vesta's density, Russell et al., 2012); and ρ = Vesta's density (3.456 kg/m^3 , Russell et al., 2012). Re-arranging Eq. (1) yields an impactor radius on the order of 1000 m. Thus, the approximate volume of this impactor is $\sim 6.8 \times 10^9 \text{ m}^3$, the mass is $\sim 2.1 \times 10^{13} \text{ kg}$ and the energy is $\sim 1.7 \times 10^{20} \text{ J}$. The approximate energy to melt the volume of subsurface ice required to form the curvilinear system in Cornelia, is found by:

$$Q = (mc\Delta T)_{\text{ice}} + (mL)_{\text{ice}} \quad (2)$$

where Q = energy in J; m = mass of water/ice to form the curvilinear system (10^{11} kg , found using a water volume of 10^8 m^3 (see Section 5.1.2) and a density of 1000 kg/m^3); c = specific heat capacity of ice ($2110 \text{ Jkg}^{-1} \text{ K}^{-1}$); ΔT = ice melting temperature – average surface temperature (128 K); and L = latent heat of fusion of ice ($3.335 \times 10^5 \text{ J/Kg}$). Thus, $\sim 6 \times 10^{16} \text{ J}$ is required to melt the ice that provides the water to form the curvilinear system; this is 0.04% of the energy of the Cornelia-forming impactor.

5.1.2. Volume

For Cornelia, we calculate that at least $\sim 10^7$ – 10^8 m^3 of water is necessary to form the curvilinear system and pitted terrain. This volume is found from three independent calculations below. Furthermore, this volume leads to a bulk subsurface ice-bearing deposit concentration of $\sim (1 \times 10^{-5})$ – (1×10^{-6}) , when the total pre-impact volume of subsurface material around and within Cornelia crater is defined as a cuboid whose edges are at a distance of one Cornelia crater radii from the crater edges.

5.1.2.1. Volume necessary to erode the curvilinear gullies Flow rate, Q (m^3/s) is given by:

$$Q = vwd \quad (3)$$

where v = flow velocity; w = gully width; and d = water depth (Heldmann et al., 2005).

Gullies are not visible in the topographic profiles, thus their depth must be <50 m (see Section 2). Additionally, since the gullies appear to be shallowly incised (Fig. 3), a conservative approximate gully depth of ~10 m is used. 10 m is also used as the approximate water depth. The average gully width is ~30 m. Assuming the gullies formed in a debris-flow-like process, the flow velocity at a cross section across a gully (Anderson and Anderson, 2010) is given by:

$$v = (Rg \sin \beta)^{1/2} \quad (4)$$

where v = mean fluid velocity; R = radius of curvature of bend (average of 154 m); g = gravitational acceleration (0.25 m/s^2); and

β = cross-channel slope of the debris flow surface as it rounds the bend (average of 29°). Thus, the average velocity of debris flows in Cornelia is on the order of 4 m/s. Consequently, the approximate flow rate for one gully in Cornelia is $\sim 1300 \text{ m}^3/\text{s}$. Estimating that one gully forms in ~ 4 min (see Section 5.1.3.1) gives a volume of $\sim 3 \times 10^5 \text{ m}^3$ of water in one gully. We mapped 357 gullies in Cornelia, so the total water volume necessary to erode all the gullies is on the order of at least $1 \times 10^8 \text{ m}^3$.

5.1.2.2. Volume necessary to form the lobate deposits Assuming that the lobate deposits form in a debris-flow like process, they once contained 10%–30% water (Malin and Edgett, 2000). Thus, a conservative volume (10%) of water in lobate deposits is given by:

$$V = 0.1Ad \quad (5)$$

where V = water volume; A = lobate deposit area; and d = lobate deposit thickness (Malin and Edgett, 2000). In Cornelia, the area of the lobate deposits is $3.4 \pm 0.5 \times 10^7 \text{ m}^2$. The gullies are not visible in the topographic profiles, thus their depth must be < 50 m (see Section 2). A conservative thickness value of 10 m is used. Accordingly, the volume of the lobate deposits is at least $3.4 \pm 0.5 \times 10^7 \text{ m}^3$.

5.1.2.3. Volume from approximate volume of pitted terrain An upper bound of the volume of water necessary to form the pitted terrain can be estimated if we assume the entire volume of the pitted terrain contains water. Assuming that the pitted terrain formed a perfectly spherical cap at the bottom of Cornelia crater, the volume is given by:

$$V = (\pi/6)(3r^2 + h^2)(h) \quad (6)$$

where V = spherical cap volume; r = spherical cap radius (approximate pitted terrain radius); and h = spherical cap height. The average height is found by drawing the trace of the expected profile of Cornelia over the actual profile of Cornelia, which has a roughly flat base due to the pitted terrain. The average height difference between the different profiles is ~ 100 m. Thus, an estimate of water volume in the pitted terrain is on the order of $6 \times 10^8 \text{ m}^3$.

5.1.3. Timescales

5.1.3.1. Timescale of gully formation We further estimate that gullies could have formed in a minimum of ~ 4 min, since the average gully length in Cornelia is 930 m and water flowing at ~ 4 m/s (see Section 5.1.2.1) reaches the end of a 930 m gully in ~ 4 min.

5.1.3.2. Timescale of crater formation In order for curvilinear systems to be preserved, they must have formed after the contact and compression, excavation and modification stages of crater formation were complete. The timescale of the contact and compression stage is $\sim 6 \times 10^{-1}$ s, found by use of the expression from Melosh (2011):

$$t_{cc} \sim L/v_i \quad (7)$$

where t_{cc} = duration of contact and compression; L = Cornelia-forming projectile diameter (2348 m); and v_i = Cornelia-forming impactor velocity (4000 m/s, see Section 5.1.1). We find that the excavation stage lasts for ~ 4 min, by use of the expression from Melosh (2011):

$$t_{ex} \sim (D/g)^{1/2} \quad (8)$$

where t_{ex} = duration of excavation; D = Cornelia diameter (15000 m), g = gravitational acceleration of Vesta (0.25 m/s^2). We find that the timescale of the modification stage is ~ 12 – 16 min, because the modification stage is a few times the length of the

excavation stage (Melosh, 2011). Thus, curvilinear systems could be preserved from ~ 20 min after the initial impact. Furthermore, since the average curvilinear gully can be formed in a minimum of ~ 4 min, the presence of transient water is required for at least ~ 24 min to form curvilinear systems.

5.2. Experiments

We conducted preliminary laboratory experiments focusing on the evaporation rate of water at low pressures, as a test of whether water could transiently survive on the surface of Vesta for the ~ 24 min required to form curvilinear systems. We used a 21.2 ft³ custom Kurt J. Lesker environmental vacuum chamber in the Extraterrestrial Materials Simulation Laboratory in the Jet Propulsion Laboratory, California Institute of Technology. Approximately 25 ml of water was placed in glass vessels of a variety of shapes and volumes to test for edge effects. AGSCO 100–170 μm glass beads, in a 4:1 ratio with the water, were added in later experiments to simulate entrained regolith. We used LabVIEW to record the pressure and temperature inside the chamber and the temperature inside the vessel.

We conducted the experiments with ~ 293 K water. While the average, undisturbed surface temperature of Vesta is ~ 145 K (Stubbs and Wang, 2012), in our proposed scenario impact-induced heating would raise the temperature to above ~ 273 K, to induce melting of subsurface ice-bearing deposits. Furthermore, simulations of the impact cratering process on Mars have shown that post-impact fluid temperatures much greater than ~ 293 K can persist for thousands of years (e.g. Barnhart et al., 2010). While this result is not directly applicable to impacts on Vesta, because of lower vestan impact velocities, it suggests that the use of ~ 293 K water is reasonable for conditions immediately post-impact.

In addition, we used pressures of $\geq 10^{-3}$ atm during these preliminary experiments. While Vesta normally has no atmosphere, an impact into subsurface ice-bearing deposits may create a transient atmosphere that exists during the formation of curvilinear gullies. For example, modeling of a cometary impact into the Moon finds that an impact-induced transient atmosphere can exist for a couple of hours (Prem et al., in press). Formation of a similar transient atmosphere on Vesta would result in greater than normal surface pressures. However, any transient atmosphere would likely be $< 10^{-3}$ atm, so further reduction of the experimental pressures are necessary.

Our preliminary results show that under the aforementioned pressure and temperature conditions, 25 ml of water in a 250 ml beaker takes ~ 150 min to evaporate. The addition of glass beads to the 25 ml of water in a 4:1 ratio simulates the entrained particles in a debris flow. This mixture evaporates in ~ 300 min, suggesting that the addition of particles decreases the evaporation rate. Thus, our preliminary experimental results indicate that under post-impact conditions, water may be able to transiently survive on the surface of Vesta for the ~ 24 min required to form curvilinear systems. We will test our hypothesis by future experiments in which a mixture of water and particles will flow, which is more representative of the proposed debris-flow-like process, and by further lowering the ambient pressure to approach transient atmosphere conditions.

6. Implications and conclusions

Since craters hosting curvilinear systems and pitted terrain are relatively young ($<$ hundreds of Ma), the inferred ice-bearing deposits may still exist within Vesta's subsurface. However, subsurface ice-bearing deposits, if present, would be too deeply buried to be detected by the VIR and GRaND instruments; ice is stable at depths of greater than a few meters within the regolith (Stubbs

and Wang, 2012) but VIR and GRaND collect data from the surface and top few centimeters of regolith (De Sanctis et al., 2011; Prettyman et al., 2011).

Additionally, we infer that formation of curvilinear systems by water from impact-heated ice-bearing deposits may have occurred throughout Vesta's history. This inference is consistent with indications of > 4.4 Ga water activity (Treiman et al., 2004) and with our observation of increased degradation of curvilinear systems in older craters, implying that curvilinear systems older than 100s Ma may have been entirely erased by later mass-wasting processes.

The proposed formation of gullies by transient water flow in a debris-flow-like process is one of the many examples of planetary-type processes on Vesta. This process is consistent with the newly expanded understanding of the distribution and behavior of water on other differentiated bodies, such as Earth's Moon (Saal et al., 2008), and elsewhere in the asteroid belt (Küppers et al., 2014; Hsieh and Jewitt, 2006). Taken together, these studies indicate that the solar system does not entirely consist of end-member bodies, either lacking or rich in water, but consists of a continuum of bodies with many intermediate states of hydration.

Acknowledgements

We thank B.W. Denevi and D.L. Buczkowski for helpful discussions and comments and K. Otto and D.P. O'Brien for assistance with calculations. We thank the Dawn team for the development, cruise, orbital insertion and operations of the Dawn spacecraft at Vesta. The data used in this paper are available from the website <http://dawndata.igpp.ucla.edu>.

References

- Ammannito, E., et al., 2013. Olivine in an unexpected location on Vesta's surface. *Nature* 504, 122–125.
- Anderson, R.S., Anderson, S.P., 2010. *Geomorphology: The Mechanics and Chemistry of Landscapes*. Cambridge University Press, New York.
- Barnhart, C.J., Nimmo, F., Travis, B.J., 2010. Martian post-impact hydrothermal systems incorporating freezing. *Icarus* 208, 101–117.
- Barrat, J.A., et al., 2011. Possible fluid–rock interactions on differentiated asteroids recorded in eucritic meteorites. *Geochim. Cosmochim. Acta* 75, 3839–3852.
- Blair, T.C., 1999. Cause of dominance by sheetflood vs. debris-flow processes on two adjoining alluvial fans, Death Valley, California. *Sedimentology* 46, 1015–1028.
- Bray, V.J., et al., 2010. New insight into lunar impact melt mobility from the LRO camera. *Geophys. Res. Lett.* 37 (L21202), 1–5.
- Britt, D.T., Consolmagno, G.J., 2004. Meteorite porosities and densities: a review of trends in the data. *Lunar Planet. Sci. Conf. Abstr.* 35, 2108.
- Buczkowski, D.L., et al., 2012. Large-scale troughs on Vesta: a signature of planetary tectonics. *Geophys. Res. Lett.* 39 (L18205), 1–6.
- Buczkowski, D.L., et al., 2014. The unique geomorphology and physical properties of the Vestalia Terra plateau. *Icarus* 244, 89–103.
- Capria, M.T., et al., 2014. Vesta surface thermal inertia properties. *Geophys. Res. Lett.* 41, 1438–1443.
- Carr, M.H., 2012. The fluvial history of Mars. *Philos. Trans. R. Soc. Lond. A* 370, 2193–2215.
- Denevi, B.W., et al., 2012. Pitted terrain on Vesta and implications for the presence of volatiles. *Science* 338, 246–249.
- Denevi, B.W., et al., 2014. The preservation and geologic effects of exogenic and hydrated materials on Vesta. In: *Vesta in the Light of Dawn: First Exploration of a Protoplanet in the Asteroid Belt*, p. 2029.
- De Sanctis, M.C., et al., 2011. The VIR spectrometer. *Space Sci. Rev.* 163, 329–369.
- De Sanctis, M.C., et al., 2012. Detection of widespread hydrated minerals on Vesta by the VIR imaging spectrometer on board the Dawn mission. *Astrophys. J. Lett.* 758, 1–5.
- De Sanctis, M.C., et al., 2014. Compositional evidence of magmatic activity on Vesta. *Geophys. Res. Lett.* 41, 3038–3044.
- Diniaga, S., Byrne, S., Bridges, N.T., Dundas, C.M., McEwen, A.S., 2010. Seasonality of present-day Martian dune-gully activity. *Geology* 38, 1047–1050.
- Diniaga, S., et al., 2013. A new dry hypothesis for the formation of martian linear gullies. *Icarus* 225, 526–537.
- Dundas, C.M., Diniaga, S., Hansen, C.J., Byrne, S., McEwen, A.S., 2012. Seasonal activity and morphological changes in martian gullies. *Icarus* 220, 124–143.
- Formisano, M., et al., 2013. The heating history of Vesta and the onset of differentiation. *Meteorit. Planet. Sci.* 48, 2316–2332.
- Fu, R.R., Elkins-Tanton, L.T., 2014. The fate of magmas in planetesimals and the retention of primitive chondritic crusts. *Earth Planet. Sci. Lett.* 390, 128–137.
- Gaskell, R.W., 2012. SPC shape and topography of Vesta from DAWN imaging data. In: *American Astronomical Society, Division of Planetary Sciences Meeting 44*. Abstract 209.03.
- Hauber, E., et al., 2011. Landscape evolution in Martian mid-latitude regions: insights from analogous periglacial landforms Svalbard. *Geol. Soc. (Lond.) Spec. Publ.* 356, 111–131.
- Heldmann, J.L., et al., 2005. Formation of Martian gullies by the action of liquid water flowing under current Martian environmental conditions. *J. Geophys. Res.* 110, E05004.
- Herrin, J.S., Zolensky, M.E., Cartwright, J.A., Mittlefehldt, D.W., Ross, D.K., 2011. Carbonaceous chondrite-rich howardites: the potential for hydrous lithologies on the HED parent. *Lunar Planet. Sci. Conf. Abstr.* 42, 2806.
- Hiesinger, H., et al., 2014. Investigating Vesta's Marcia crater with Dawn data. In: *Eur. Planet. Sci. Congress*. In: *EPSC Abstracts*, vol. 9, p. 509.
- Holsapple, K.A., Housen, K.R., 2007. A crater and its ejecta: an interpretation of deep impact. *Icarus* 187, 345–356.
- Hsieh, H.H., Jewitt, D., 2006. A population of comets in the main asteroid belt. *Science* 312, 561–563.
- Hugenholtz, C.H., 2008. Frosted granular flow: a new hypothesis for mass wasting in martian gullies. *Icarus* 197, 65–72.
- Jaumann, R., et al., 2012. Vesta's shape and morphology. *Science* 336, 687–690.
- Jaumann, R., et al., 2014. The geological nature of dark material on Vesta and implications for the subsurface structure. *Icarus* 240, 3–19.
- Johnsson, A., et al., 2014. Evidence for very recent melt-water and debris flow activity in gullies in a young mid-latitude crater on Mars. *Icarus* 235, 37–54.
- Keil, K., 2002. Geological history of asteroid 4 Vesta: the "Smallest Terrestrial Planet". *Asteroids III*, 573–584.
- Knauth, L.P., Burt, D.M., 2002. Eutectic brines on Mars: origin and possible relation to young seepage features. *Icarus* 158, 267–271.
- Kumar, P.S., Head, J.W., Kring, D.A., 2010. Erosional modification and gully formation at Meteor Crater, Arizona: insights into crater degradation processes on Mars. *Icarus* 208, 608–620.
- Kumar, P.S., et al., 2013. Gullies and landslides on the Moon: evidence for dry-granular flows. *J. Geophys. Res., Planets* 118, 1–18.
- Küppers, M., et al., 2014. Localized sources of water vapour on the dwarf planet (1) Ceres. *Nature* 505, 525–527.
- Le Corre, L., et al., 2013. Olivine or impact melt: nature of the "Orange" material on Vesta from Dawn. *Icarus* 226, 1568–1594.
- Malin, M.C., Edgett, K.S., 2000. Evidence for recent groundwater seepage and surface runoff on Mars. *Science* 288, 2330–2335.
- McCord, T.B., et al., 2012. Dark material on Vesta from the infall of carbonaceous volatile-rich material. *Nature* 491, 83–86.
- McSween, H.Y., et al., 2011. HED meteorites and their relationship to the geology of Vesta and the Dawn mission. *Space Sci. Rev.* 163, 141–174.
- Mellon, M.T., Phillips, R.J., 2001. Recent gullies on Mars and the source of liquid water. *J. Geophys. Res.* 106, 23165–23179.
- Melosh, H.J., 2011. *Planetary Surface Processes*. Cambridge University Press, New York.
- Mouginis-Mark, P.J., Garbeil, H., 2007. Crater geometry and ejecta thickness of the Martian impact crater Tooting. *Meteorit. Planet. Sci.* 42, 1615–1625.
- Musselwhite, D.S., Swindle, T.D., Lunine, J.I., 2001. Liquid CO₂ breakout and the formation of recent small gullies on Mars. *Geophys. Res. Lett.* 28, 1283–1285.
- Newsom, H.E., et al., 1986. Fluidization and hydrothermal alteration of the suevite deposit at the Ries crater, west Germany, and implications for Mars. *J. Geophys. Res.* 91, E239–E251.
- O'Brien, D.P., Sykes, M.V., 2011. The origin and evolution of the asteroid belt – implications for Vesta and Ceres. *Space Sci. Rev.* 163, 41–61.
- Osinski, G.R., 2004. Impact melt rocks from the Ries structure, Germany: an origin as impact melt flows? *Earth Planet. Sci. Lett.* 226, 529–543.
- Phillips, L.F., Schumm, S.A., 1987. Effect of regional slope on drainage networks. *Geology* 15, 813–816.
- Prem, P., et al., in press. Transport of water in a transient impact-generated lunar atmosphere. *Icarus*. <http://dx.doi.org/10.1016/j.icarus.2014.10.017>.
- Prettyman, T.H., et al., 2011. Dawn's gamma ray and neutron detector. *Space Sci. Rev.* 163, 371–459.
- Prettyman, T.H., et al., 2012. Elemental mapping by Dawn reveals exogenic H in Vesta's regolith. *Science* 338, 242–246.
- Preusker, F., et al., 2012. Topography of asteroid (4) Vesta from Dawn FC HAMO stereo images. In: *Geophys. Res. Abstracts*, vol. 14. Eur. Geosci. Union, 11805.
- Raymond, C.A., et al., 2013. Vestalia terra: an ancient mascon in the southern hemisphere of Vesta. *Lunar Planet. Sci. Conf. Abstr.* 44, 2882.
- Reddy, V., et al., 2012a. Delivery of dark material to Vesta via carbonaceous chondritic impacts. *Icarus* 221, 544–559.
- Reddy, V., et al., 2012b. Color and Albedo heterogeneity of Vesta from Dawn. *Science* 336, 700–704.
- Reiss, D., Erkeling, G., Bauch, K.E., Hiesinger, H., 2010. Evidence for present day gully activity on the Russell crater dune field, Mars. *Geophys. Res. Lett.* 37, L06203.
- Russell, C.T., et al., 2012. Dawn at Vesta: testing the protoplanetary paradigm. *Science* 336, 684–686.

- Russell, C.T., et al., 2014. Lessons from Vesta and Ceres. *Eur. Planet. Sci. Congress* 18.
- Saal, A.E., et al., 2008. Volatile content of lunar volcanic glasses and the presence of water in the Moon's interior. *Nature* 454, 192–195.
- Sarafian, A.R., Roden, M.F., Patiño-Douce, A.E., 2013. The volatile content of Vesta: clues from apatite in eucrites. *Meteorit. Planet. Sci.* 48 (11), 2135–2154.
- Schenk, P., et al., 2012. The geologically recent giant impact basins at Vesta's South Pole. *Science* 336, 694–697.
- Schon, S.C., Head, J.W., 2011. Keys to gully formation processes on Mars: relation to climate cycles and sources of meltwater. *Icarus* 213, 428–432.
- Schon, S.C., Head, J.W., 2012. Gasa impact crater, Mars: very young gullies formed from impact into latitude-dependent mantle and debris-covered glacier deposits? *Icarus* 218, 459–477.
- Scully, J.E.C., et al., 2014. Geomorphology and structural geology of Saturnalia Fossae and adjacent structures in the northern hemisphere of Vesta. *Icarus* 244, 23–40.
- Shinbrot, T., Duong, N.H., Kwan, L., Alvarez, M.M., 2004. Dry granular flows can generate surface features resembling those seen in Martian gullies. *Proc. Natl. Acad. Sci. USA* 101, 8542–8546.
- Sierks, H., et al., 2011. The dawn framing camera. *Space Sci. Rev.* 163, 263–327.
- Stewart, S.T., Nimmo, F., 2002. Surface runoff features on Mars: testing the carbon dioxide formation hypothesis. *J. Geophys. Res.* 107, 5069–5081.
- Stubbs, T.J., Wang, Y., 2012. Illumination conditions at the Asteroid 4 Vesta: implications for the presence of water ice. *Icarus* 217, 272–276.
- Tornabene, L.L., et al., 2012. Widespread crater-related pitted materials on Mars: further evidence for the role of target volatiles during the impact process. *Icarus* 220, 348–368.
- Tosi, F., et al., 2014. Thermal measurements of dark and bright surface features on Vesta as derived from Dawn/VIR. *Icarus* 240, 36–57.
- Treiman, A.H., 2003. Geologic settings of Martian gullies: implications for their origins. *J. Geophys. Res.* 108, 8031–8044.
- Treiman, A.H., Lanzirotti, A., Xirouchakis, D., 2004. Ancient water on asteroid 4 Vesta: evidence from a quartz veinlet in the Serra de Mage eucrite meteorite. *Earth Planet. Sci. Lett.* 219, 189–199.
- Turrini, D., Svetsov, V., 2014. The formation of Jupiter, the Jovian early bombardment and the delivery of water to the asteroid belt: the case of (4) Vesta. *Life* 4, 4–34.
- Warren, P.H., Isa, J., Gessler, N., 2013. Petrology of secondary mineral development, probably fluid-driven, within the uniquely evolved Eucrite Northwest Africa 5739. *Lunar Planet. Sci. Conf. Abstr.* 44, 2875.
- Williams, D.A., et al., 2014a. Lobate and flow-like features on asteroid Vesta. *Planet. Space Sci.* 103, 24–35.
- Williams, D.A., et al., 2014b. The geology of the Marcia quadrangle of asteroid Vesta: assessing the effects of large, young craters. *Icarus* 244, 74–88.